[4]T. B. Johansson, R. E. Van Grieken, J. W. Nelson, and J. W. Winchester, Anal. Chem. 47, 855 (1975).
[5]B. Jensen and J. W. Nelson, Nucl. Instrum. Methods 71, 137 (1971).
[6]D. C. Camp, A. L. van Lehn, J. R. Rhodes, and A. H. Pradzynski, J. X-Ray Spectrom. 4, 123 (1975).
[7]J. A. Bearden and A. F. Burr, *X-Ray Wavelengths and X-Ray Atomic Energy Levels*, U. S. National Bureau of Standards Special Publication No. NSRDS-NBS14 (U.S. GPO, Washington, D.C., 1967).
[8]T. A. Carlson, C. W. Nestor, F. B. Malik, and T. C. Tucker, Nucl. Phys. A135, 57 (1969); C. C. Lu, F. B. Malik, and T. A. Carlson, Nucl. Phys. A175, 289 (1971).
[9]G. Presser, Phys. Lett. 56A, 273 (1976).
[10]E. Storm and H. I. Israel, Nucl. Data, Sect. A 7, 565 (1970); R. Anholt and J. O. Rasmussen, Phys. Rev. A 9, 585 (1974).
[11]R. K. Wyrick and T. A. Cahill, Phys. Rev. A 8, 2288 (1973); R. G. Flocchini, thesis, University of California, Davis, 1974 (unpublished).
[12]J. C. Franklin and L. Landau, private communication.
[13]W. H. Christie and D. H. Smith, private communication; S. S. Cristy and J. F. McLaughlin, private communication.

# Experimental Determination of the Charge Density of the Bond-Forming Electrons in $N_2$ †

M. Fink, D. Gregory, and P. G. Moore*
*Physics Department and Electronics Research Center, The University of Texas, Austin, Texas 78712*
(Received 22 April 1976)

High-precision total differential scattering cross sections for 40-keV electrons incident on $N_2$ have been measured. In order to observe binding effects in the scattering cross sections, the data have been compared to a theoretical set of intensities based on scattering from noninteracting nitrogen atoms placed in the proper geometric relation. The resulting difference function has been Fourier transformed according to the procedures described by Kohl and Bartell. The charge-density-difference map which is the result of this deconvolution process is compared with the Hartree-Fock model.

During the last few years, a new electron diffraction unit utilizing counting techniques has been designed and built at the University of Texas at Austin. The unit was conceptually based on a unit described by Fink and Bonham[1] and by Bonham and Fink[2] and will be described in detail in another publication.[3] Two major improvements have been achieved; the present uncertainty in the scattering angle is ±2 arc sec, and the scattered intensity is recorded with an average of 0.1%. The resulting data for 40-keV electrons incident on $N_2$ are of sufficient accuracy to warrant, for the first time, a critical comparison between theoretical predictions of bonding-electron rearrangement in molecules and the corresponding experimental results. An experimental charge-density map showing this bonding-electron rearrangement has been constructed, and is compared to the Hartree-Fock model (which appears to be inadequate to describe certain features found in the experimental charge-density map). Even if the necessary assumptions in the development of the charge-density map prove to be faulty, future theoretical charge densities, when transformed to scattering cross sections, can be directly compared to the present data.

Experimental scattered intensities, generally expressed in terms of the Rutherford cross section as $s^4I(s)$, may be compared to theory by subtracting the scattered intensities predicted by the independent-atom model (IAM), i.e., the scattering from a molecule made of noninteracting atoms in the proper geometric arrangement with vibrational and rotational averaging taken into account. The difference between the experiment and the model calculation is called a $\Delta\sigma$ function and can be expressed theoretically for $N_2$ in terms of the atomic charge densities as

$$\Delta\sigma(s)=\tfrac{1}{16}(\pi a_0^2)s^4(I_{\mathrm{exp}}-I_{\mathrm{theor}})=-2Z\int_0^\infty r^2\Delta\rho(r)j_0(sr)\,dr+\int_0^\infty r^2\Delta\rho_c(r)j_0(sr)\,dr\,, \tag{1}$$

where $s=(4\pi/\lambda)\sin\theta/2$ is the momentum transfer, $Z$ is the atomic number, and $\Delta\rho(r)$ and $\Delta\rho_c(r)$ are the radial parts of, respectively, the electron-nuclear and electron-electron charge-difference functions reflecting the rearrangement of the charge densities when the chemical bond is formed.

The transformation from the momentum space in which the cross section is determined to real space

which contains the density functions is not straightforward because of the rotational and vibrational averaging of the target molecule. A study by Kohl and Bartell,[4] however, showed that, given a reasonable functional form for the charge density, the averaging and the Fourier transform can be accomplished analytically. If the charge-density difference function for a homonuclear diatomic molecule is expressed in the form

$$\Delta\rho(\vec{r}) = \sum_n \sum_k a_{nk} r^k \exp(-\lambda_{nk} r) P_n(\cos\theta) + \sum_n \sum_k a_{nk} (r')^k \exp(-\lambda_{nk} r') P_n(\cos\theta'), \quad (2)$$

where the definitions of $r$, $r'$, $\theta$, $\theta'$, are shown in the inset of Fig. 2, the resulting $\Delta\sigma$ function (taking the averages into account) is given by

$$\Delta\sigma(s) = -16\pi Z \{ g_0(s)[1 + j_0(sr_{AB}) \exp(-l^2 s^2/2)] + \sum_{n>0} g_n(s) j_n(sr_{AB}) \exp(-l^2 s^2/2) \}, \quad (3)$$

where

$$g_n(s) = (2s)^n n! \sum_k a_{nk} (-d/d\lambda_{nk})^{k-n+1} (s^2 + \lambda_{nk}^2)^{-n-1}$$

and the $a$'s and the $\lambda$'s are free parameters.

In order to take advantage of this study in the evaluation of the present data, the following approximation, which may be crucial, has to be adopted: Because of the $2Z$ weight factor of the electron-nuclear charge-density distribution, the electron-electron contribution can be neglected. This is an *a priori* approximation and can only be justified by future studies of model calculations.

Eight measurements were made with $N_2$ as the target gas spanning the $s$ range of 1.1 to 20.0 $Å^{-1}$. The different sets of data were scaled to each other by matching $s^4I$ and then put on an absolute level by matching to an IAM cross section calculated from partial-wave atomic scattering factors and the configuration-interaction inelastic scattering factors from Naon and Cornille.[5] From the kinematics of the scattering process, the bond length and rms amplitude of vibration of $N_2$ have been determined to be 1.0976 and 0.0319 Å, respectively, where the total uncertainty in the fit of the model to the data is 0.2%. These structure parameters were used to calculate the reference $s^4I$ values.

Figure 1 shows the cross-section difference function $\Delta\sigma$, as defined in Eq. (1). According to a study by Tavard,[6] the net area under this curve has to be equal to the binding energy of nitrogen (9.8 eV) reduced by the energy already taken care of in the IAM (7.1 eV). The value determined in this study for the binding energy of nitrogen is 12.6 eV. This value is somewhat high, but it reflects the progress made since previous values[7] determined by the same method were 22.6 and

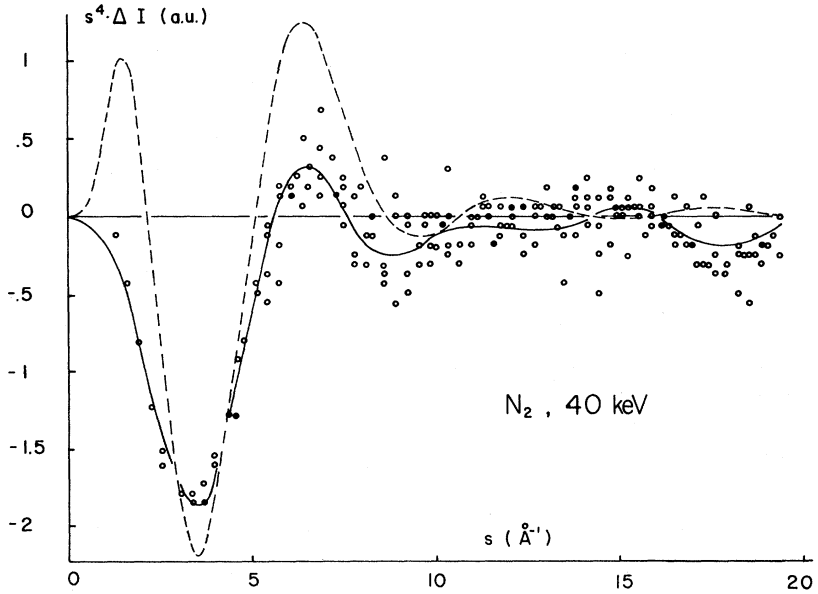


FIG. 1. $\Delta\sigma$ curve, difference between the experimental differential cross section and theoretical values based on the independent-atom model. The solid line represents the analytic fit to the data utilizing Eq. (3). The dashed line is the $\Delta\sigma$ curve employing molecular Hartree-Fock and atomic Hartree-Fock wave functions.

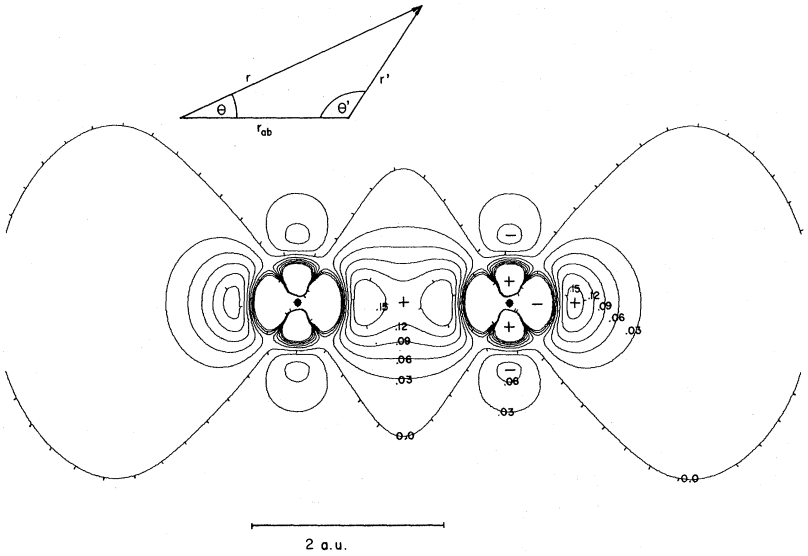


FIG. 2. Deconvoluted charge-density difference map based on the analytic fit to experimental data. The density is in electrons per $a_0^3$. The inset defines the coordinate system used.

24.8 eV.

The $\Delta\sigma$ curve has been fitted in Eq. (3) and the solid curve in Fig. 1 presents the function obtained with a nonlinear least-squares procedure. Two $n=2$, $k=1$ terms were necessary in order to obtain the best fit. The parameters in Eq. (4) were determined to be

$$a_{00}=5.0, \quad \lambda_{00}=30.5,$$
$$a_{01}=-0.93, \quad \lambda_{01}=4.15,$$
$$a_{02}=4.97, \quad \lambda_{02}=5.78,$$
$$a_{11}=4.93, \quad \lambda_{11}=11.82,$$
$$a_{21}=-160.0, \quad \lambda_{21}=11.97,$$
$$a_{21}=-3.92, \quad \lambda_{21}=3.94.$$

When those parameters (given in atomic units) are inserted in Eq. (2), an atomic charge-density difference map can be generated, and this map is shown in Fig. 2. For comparison, a map was constructed utilizing the molecular Hartree-Fock (HF) wave function of Bader, Henneker, and Cade[8] and the HF nitrogen atom. Thus, Fig. 3 shows the rearrangement of the atomic electrons in forming the bond, as predicted by a HF calculation. A comparison of Figs. 2 and 3 shows several similarities between theory and experiment but also some rather striking differences. In both functions the $j_2$ term strongly dominates the behavior of $\Delta\rho(r)$. There is an electron charge-density enrichment of equal amounts in the two cases between the atoms to form the bond. The main difference lies in the appearance of two rings of charge gain centered around the internuclear axis in the experimental figure. The charge required to build up this ring structure is mostly drawn from the area immediately surrounding the nuclei. A comparison of the $\Delta\sigma$ curves (measured and calculated by HF molecular wave functions) shows which special feature can be responsible for the appearance of charge

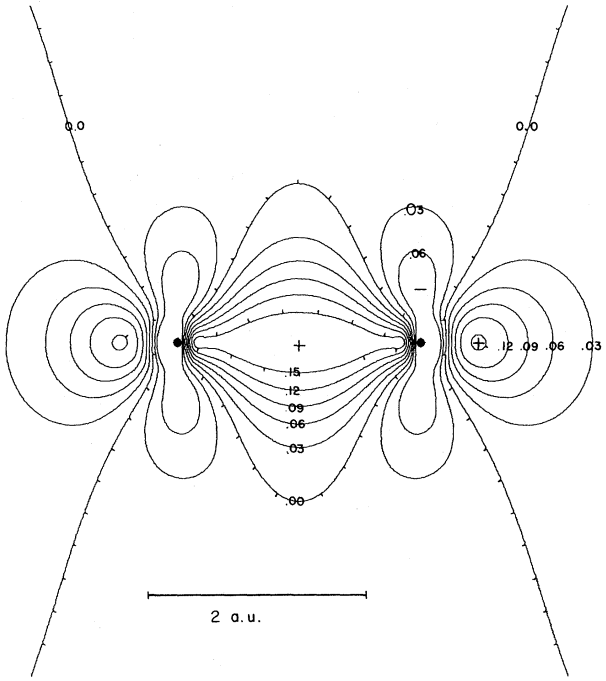


FIG. 3. Charge-density difference map reproduced from Ref. 4 using molecular Hartree-Fock and atomic Hartree-Fock wave functions.

rings at these positions in the molecule. The $\Delta\sigma$ curves disagree rather strongly near the maximum at $s = 8$ Å$^{-1}$. In order to fit the experimental curve, two $j_2$ terms with opposite signs and very different damping factors ($\lambda$) are required to eliminate the natural $j_2$ peak at $s = 8$ Å$^{-1}$, while the theoretical curve allows the $j_2$ to reach this maximum. A detailed analysis shows that it is the coupling between the two $j_2$ terms which generates the two rings in the experimental $\Delta\sigma$ function.

At present, highly accurate differential cross sections can be measured for gaseous targets. With the adoption of the approximation that $\Delta\rho_c \ll 2Z\Delta\rho$ the data can be transformed into charge-density difference functions. A comparison with HF calculations shows good overall agreement with the exception of two weak rings of charge. These rings reflect either the importance of $\Delta\rho_c(r)$ or the influence of the $\pi_g^2, \pi_u^2$ interaction on the bond. However, a configuration interaction calculation should be able to confirm the ring structure in $\Delta\rho$.

†This research was supported by the R. A. Welch Foundation and by the Department of Defense Joint Services Electronics Program through the U. S. Air Force Office of Scientific Research Contract No. F44620-71-C-0091.

*Present address: Naval Research Laboratory, Washington, D. C. 20390.

[1]M. Fink and R. A. Bonham, Rev. Sci. Instrum. 41, 389 (1970).

[2]R. A. Bonham and M. Fink, *High Energy Electron Scattering* (Van Nostrand, New York, 1974), Chap. 3.

[3]M. Fink, P. G. Moore, and D. Gregory, "Precise Determination of Differential Electron Scattering Cross Sections I. The Apparatus and $N_2$ Results" (to be published).

[4]D. A. Kohl and L. S. Bartell, J. Chem. Phys. 51, 2891 (1969).

[5]M. Naon and M. Cornille, J. Phys. B 5, 1965 (1972).

[6]C. Tavard, Cah. Phys. 20, 397 (1965).

[7]M. Fink, D. A. Kohl, and R. A. Bonham, Chem. Phys. Lett. 4, 349 (1969).

[8]R. F. W. Bader, W. H. Henneker, and P. E. Cade, J. Chem. Phys. 46, 3341 (1967).

## Magnetohydrodynamic Properties of the *D*-Shaped Tokamak Controlled by Active Field Shaping

H. Toyama, K. Makishima, H. Kaneko, M. Noguchi, and S. Soshikawa*
*Department of Physics, Faculty of Science, University of Tokyo, Tokyo, Japan*
(Received 31 December 1975)

By means of active field shaping, a $D$-shaped, elongated plasma has been obtained with a maximum plasma current of 50 kA corresponding to $q = 2.4$ for the toroidal magnetic field of 2.2 kG. In this stage magnetic perturbations of $m = 2$ kinklike mode have been at high level. The disruptive instability with a negative voltage spike, an expansion of the plasma column, and an inward shift in the major radius have been observed. These magnetohydrodynamic properties are similar to those of circular cross section tokamaks.

Tokamaks with certain noncircular cross sections may introduce significant advantages relative to conventional tokamaks.[1] For an elliptical cross section with toroidal major radius $R$, major and minor semi-axes $b$ and $a$, respectively, toroidal field $B_t$, and total plasma current $I_p$, the safety factor at the plasma edge, $q_a$, is

$$q_a = \frac{2\pi a^2 B_t}{\mu_0 R I_p} \frac{1+(b/a)^2}{2}, \quad (1)$$

under the assumption of a flat current profile. With the safety factor, the toroidal magnetic field, the plasma volume, and the aspect ratio $R/a$ fixed, the plasma current and the current density of the elongated tokamak can be larger than those of the circular one by a factor

$$\kappa_1 = (a/b)^{1/3}[1+(b/a)^2]/2, \quad (2)$$

$$\kappa_2 = (a/b)^{2/3}[1+(b/a)^2]/2, \quad (3)$$

respectively. The gross magnetohydrodynamic (MHD) configurational stability in noncircular tokamaks has been studied in devices such as Doublet series,[2] Finger-Ring,[3] and Rector.[4] However, experimental data on the stability at low $q$ in the case of active field shaping are insufficient.

A device named TNT (Tokyo Noncircular Tokamak) using external shaping coils has been constructed to investigate what type of cross section makes best use of the advantages of noncircular